2016. Journal of Arachnology 44:199–209

Mechanical properties of male genitalia in *Leiobunum* harvestmen (Opiliones: Sclerosomatidae)

Mercedes Burns[1,2] and **Jeffrey W. Shultz**[1]: [1]Department of Entomology and BEES Graduate Program, University of Maryland, College Park, MD 20742; [2]Present address: Department of Biology, San Diego State University, San Diego, CA 92182. Email: mercedes.burns@gmail.com

Abstract. The morphology of arthropod intromittent organs evolves rapidly and is often species specific, phenomena widely attributed to sexual selection. Similar patterns in biomechanical properties may also exist, but practical challenges in manipulating small structures and measuring minute forces has impeded experimental biomechanical analysis. Here we describe a device that displaces a small structure while measuring its resistance, and use it to examine the biomechanics of penile flexure in the eastern North American harvestman genus *Leiobunum* C.L. Koch, 1839. Several *Leiobunum* lineages have lost primitive penis-associated nuptial-gift sacs and have gained apparent female pregenital barriers, a co-evolutionary pattern consistent with shifts from precopulatory enticement to more-antagonistic strategies. We tested for an association between losses of nuptial-gift sacs and increases in penile flexural resistance using five sacculate and five non-sacculate species. We measured three mechanical variables—resistance force, elastic efficiency and viscoelastic relaxation time—under lateral, dorsal, and ventral flexion. Our functional assumptions about sacculate and non-sacculate penes anticipated two biomechanically-defined species clusters, but three were found: a diverse sacculate group, a monophyletic non-sacculate group and an unanticipated mixed group. This work demonstrates that experimental genital biomechanics in arthropods is possible, and we discuss the functional implications of our results.

Keywords: Reproduction, viscoelasticity, elastic efficiency, phylogenetic comparative methods

Explaining the remarkable diversity of reproductive structures in arthropods and other animals is a perennial goal of evolutionary biologists (Day & Young 2004; Leonard & Cordoba-Aguilar 2010). Attention has centered on the often species-specific and sometimes exaggerated or complex traits of males (Hosken & Stockley 2004), although several recent authors have highlighted the importance of genital variation in females as well (Brennan et al. 2007; Sánchez et al. 2011; Tanabe & Sota 2013; Ah-King et al. 2014). The persistent bias toward research on male structures, especially intromittent organs, likely reflects their proven value for delimiting species (Edwards & Knowles 2014), their relatively rapid rate of evolution (Cayetano et al. 2011; Cassidy et al. 2014; Masly & Kamimura 2014), and the numerous evolutionary factors that have been invoked to explain their diversity (Leonard & Cordoba-Aguilar 2010), including female preference (Kokko et al. 2003), sperm competition (Parker et al. 2013), and cryptic female choice (Eberhard 1996; Albo et al. 2013). An understanding of the contributions that different selection mechanisms have made in shaping genitalic diversity should benefit from detailed information about the mechanical properties of genitalia (Cayetano et al. 2011), but existing information is largely based on inferences drawn from static anatomy or associated behavior rather than from experimental measurement of biomechanical variables (Bonduriansky & Day 2003; Márquez & Knowles 2007). Consequently, despite active interest in the roles of female enticement and coercion as male mating strategies, there is little information about the intrinsic ability of male intromittent organs to respond mechanically to female movement or to overcome female resistance during antagonistic interactions (but see Brennan et al. 2010). Here we focus on the mechanical properties of penes in the eastern North American species of harvestmen from the genus *Leiobunum* C.L. Koch, 1839 (Fig. 1), a clade for which reproductive diversity is increasingly well documented (Burns et al. 2012, 2013; Fowler-Finn et al. 2014; Burns & Shultz 2015).

Harvestmen are unusual among arachnids in having a true penis and in mating face to face (Machado et al. 2015; Fig. 1). The reproductive structures in both sexes are enclosed within a pregenital chamber that occupies the ventral part of the abdomen and opens anteriorly just posterior to the mouth. This chamber is enclosed ventrally by a large sclerite, the genital operculum, which articulates with the abdomen posteriorly via a transverse hinge to open and close like a trapdoor. The penis is essentially a cuticular tube that usually has a subterminal joint that divides it into a long proximal shaft and short distal glans, which has a thin terminal stylus that bears the small primary genital opening. The glans-shaft joint is operated by a bi- or multi-pinnate muscle that arises from the walls of the shaft and inserts via a long tendon on the ventral surface of the joint. The penis is externalized anteriorly by the combined effects of protractor muscles and hydraulic eversion of the flexible walls of the pregenital chamber.

Two basic types of penes have been distinguished based on the presence or absence of a subterminal pair of cuticular sacs (Fig. 1A). The sacs carry a male-generated nuptial gift that may be accessed orally by the female early in mating (Fig. 1D), a behavior that was often confused with copulation by early naturalists due to the proximity of the mouth and pregenital opening. Penile sacs were lost several times in *Leiobunum* (Burns et al. 2013); losses typically accompanied by the evolution of a sclerotized pregenital barrier in females. These correlated transformations suggest that female enticement via nuptial gifts was important in the primitive premating strategy in *Leiobunum* but was replaced multiple times by other mechanisms, including antagonistic interactions between the penis and the opening to the female pregenital chamber (Burns et al. 2013). Recent work indicates that the relative maximum forces produced by the penis protractor muscle and by the closer of the female genital operculum coevolved and are

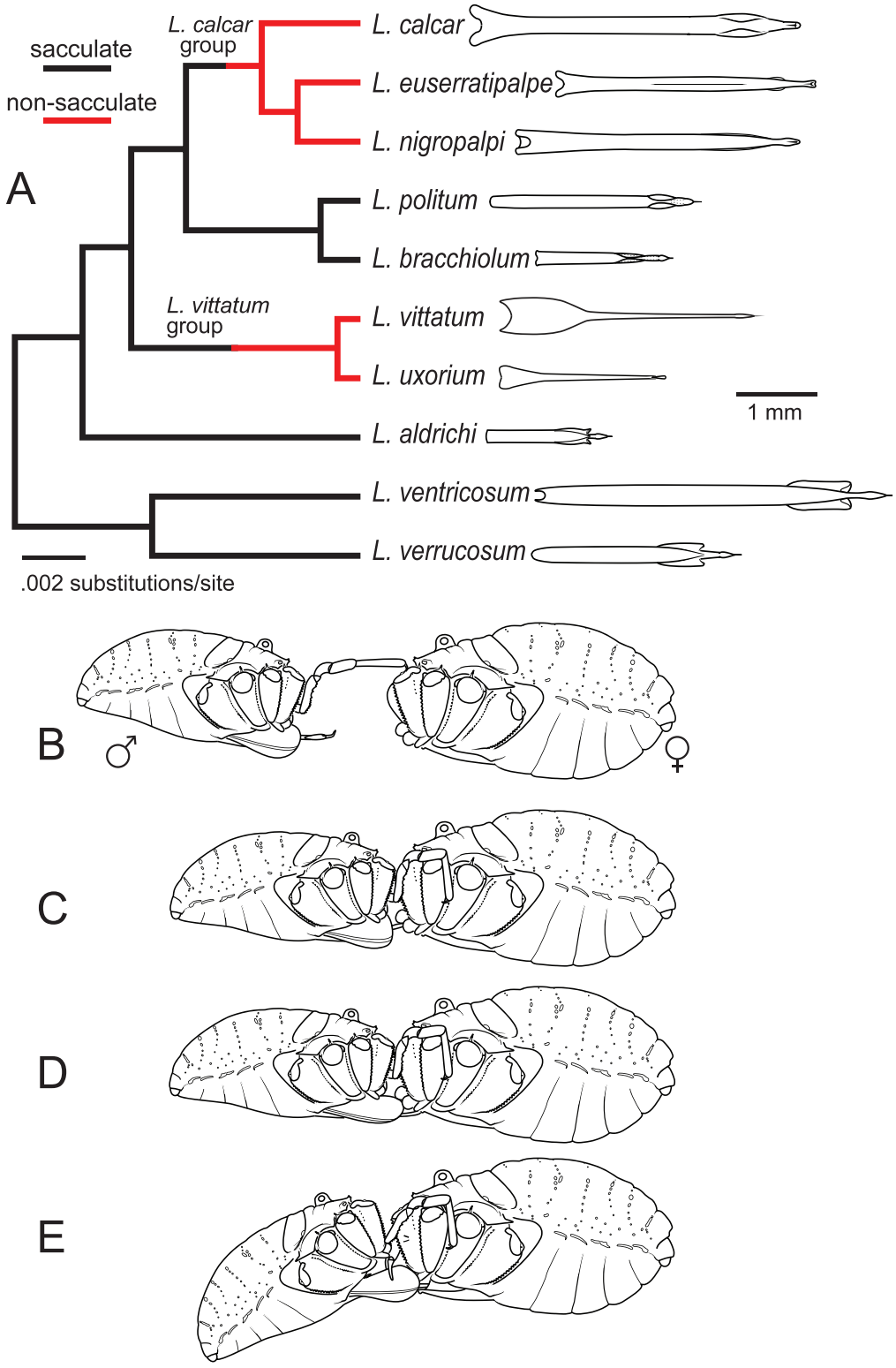

Figure 1.—Male reproductive morphology and phylogeny of *Leiobunum*. A. Penes (to same scale) from 10 *Leiobunum* species depicted on a pruned maximum clade credibility tree (Burns et al. 2013). We hypothesized that these discrete classes should be highly correlated with genital function, such that mechanical force traits might discriminate them. B–E. Mating in *Leiobunum verrucosum* (legs removed for clarity). B. Male encounters receptive female, male palps preparing to grasp female, penis extruded. C. Male clasps female with palps posterior to leg coxa II, delivers initial nuptial gift to female from penile sacs. D. Female feeds from male glands, penis lodged near female pregenital opening. E. Intromission associated with reorientation of bodies.

higher in non-sacculate species, suggesting that greater mechanical forces are produced and resisted in non-sacculate forms (Burns & Shultz 2015).

We hypothesized that the mechanical properties of penes in *Leiobunum* have changed from those that accommodate female preferences to those that can transmit or resist mechanical forces when interacting with the female's pregenital opening. Specifically, we expect penes used in forceful precopulatory interactions to resist higher bending forces than those used principally for enticing females with nuptial gifts. We also predicted changes in two parameters associated with cuticular viscoelasticity. In structures composed of ideally elastic materials, the energy used in deforming a structure is stored as elastic potential energy and recovered as kinetic energy as the penis regains its resting state, regardless of the duration or rate of loading or unloading (Vincent 2012). However, in viscoelastic materials, some energy is lost to heat during deformation, with the amount being time dependent. Thus, we also predicted that the amount and rate of energy loss would be higher in penes that are adapted to accommodate female nuptial-gift feeding and lower in penes adapted for applying large or prolonged forces to the female

We tested our hypotheses by bending penes from 10 *Leiobunum* species while measuring both flexural resistance and flexural displacement. Measurements were obtained from a phylogenetically diverse sample of five sacculate species and representatives from two non-sacculate clades, the *calcar* and *vittatum* groups (Fig. 1A). We measured three biomechanical variables—maximum resistance force for a flexural displacement of 5% of beam length, the efficiency of elastic energy storage, and the rate of viscoelastic relaxation in static bending. Phylogenetic multivariate analyses of our data recovered two species clusters (the sacculate group and monophyletic *calcar* clade) that were consistent with our biomechanical predictions but also a third cluster that was not anticipated. Ultimately, this work demonstrates that mechanical properties of reproductive structures can be measured and that data derived from these measurements can be used to test hypotheses about arthropod mating systems.

METHODS

Animals.—We examined 60 male specimens representing ten *Leiobunum* species (Fig. 1A), constituting a subset of species examined in Burns & Shultz (2015). Five species have penes with subterminal gift-bearing sacs and females that lack pregenital barriers (i.e., *L. ventricosum* (Wood, 1868), *L. verrucosum* (Wood, 1868), *L. aldrichi* Weed, 1893, *L. politum* (Weed, 1889), *L. bracchiolum* McGhee, 1977), which we term "sacculate species". Five species lack gift-bearing sacs and females have sclerotized pregenital barriers (i.e., the *vittatum* group: *L. uxorium* Crosby & Bishop, 1924, *L. vittatum* (Say, 1821) and the *calcar* group: *L. nigropalpi* (Wood, 1868), *L. euserratipalpe* Ingianni, McGhee & Shultz, 2011, *L. calcar* (Wood, 1868)), which we term "non-sacculate species". Specimens were collected and maintained up to a week in laboratory terraria with food (pulverized fish food) and water provided *ad libitum* in cotton-stoppered vials. See Table 1 for additional species information.

Apparatus.—We assembled a device to measure forces associated with penile flexural resistance and flexural displacement (deflection) in fresh harvestman penes mounted as a cantilever (Fig. 2). We attached a force transducer (Aurora Scientific, Inc.: Model 404A: range, 0-100 mN; sensitivity; 10.0 mN; resolution, 2000 nN) to a vertically mounted, computer-controlled translation stage (Thor Labs: OptoDC Servo Motor Driver #001). A displacement transducer (Microstrain: SG-DVRT-4: max. linear stroke, 24 mm; resolution, 6 μm) recorded linear movement of the force transducer. The translation stage was programmed to move at 1 mm/s. A stiff, hooked, non-magnetic wire was attached to the input tube of the force transducer and used in deflecting the penis.

Protocol.—Adult specimens were sacrificed by placing them in a freezer at –20°C for 10 minutes, after which the penis was removed and affixed at its proximal end to a round glass cover slip using ethyl cyanoacrylate gel (Super Glue®). A drop of accelerant (Turbo Set I, Palm Labs Adhesives, Inc.) was applied to the glue bead to fix the penis as a full-moment cantilever (Fig. 2B). The cover slip with attached penis was submerged in a clear-sided, open-top polyacrylic box filled with room-temperature Ringer's solution. The cover slip was affixed to the side of the box using 1/8 inch x 1/8 inch (.3175 cm × 3175 cm) neodymium magnets to facilitate repositioning (Fig. 2A).

The hooked wire from the force transducer was brought into contact with the penis at a point one third of free-penis length from the distal end. This length was selected to avoid applying force to the sac region of penes from sacculate species (Fig. 1A). The translation stage was programmed to bend the penis with a deflection of 5% of the beam length. Three consecutive hysteresis loops (Fig. 3A) were obtained from each penis, with the penis displaced and returned to its resting position at 1 mm/s. Hysteresis loops were obtained for dorsal, ventral and horizontal deflection from the resting position, as each of these flexural directions may be imposed by the female pregenital chamber upon the penis during precopulation. We also deflected each penis to 5% of beam length and held it for at least 180 s while measuring the viscoelastic relaxation of the restoring force (Fig. 3B). Displacement and force data were sampled every 50 ms using Easylogger Dual Version 1.0 software (EasySync Ltd.).

Mechanical variables.—We calculated three mechanical variables each from dorsal, ventral and lateral flexures—force at maximum experimental displacement F_{max} (or cF_{max} when corrected for body size), elastic efficiency R, and relaxation time to 90% F_{max} (T_{90})—resulting in a total of nine variables. Mean values for all variables were established for each specimen from three replicates, and mean species values were calculated from specimen means.

F_{max} is the force required to achieve a vertical deflection of the penis equal to 5% of beam length. Consequently, F_{max} can be viewed a measure of stiffness at a geometrically similar flexural displacement across specimens. To adjust the magnitude of F_{max} for body size, we derived a method of size correction from the standard equation for cantilevered beams fixed at one end (Vogel 2003):

$$FD^{-1} = 3EIL^{-3} \tag{1}$$

and its proportional representation:

$$\left[FD^{-1}\right] = EIL^{-3} \tag{2}$$

Table 1.—Taxon sampling for molecular phylogenetic reconstruction and mechanical force trait evaluation. Accession numbers are for the GenBank genetic sequence repository; numbers GQ870643–GQ870668 and GQ872152–GQ872185 are derived from Hedin et al. (2010). Column 5: penile nuptial gift sac presence, grouping variable used in testing for trait mean differences. Column 6: numbers of male specimens analyzed for mechanical force traits.

Species	GenBank accession numbers	Molecular specimen locality	Mechanical data specimen locality	Penile nuptial gift sac presence	Number of specimens
Leiobunum aldrichi	GQ870650, JQ432342, JQ432284, GQ872154, GQ870649, JQ432343, JQ432285, GQ872153, JQ432344, JQ432286, JQ432238	USA: MI: Calhoun Co.	USA: MD: Frederick Co.	Present	2
L. bracchiolum	JQ432330, JQ432272, JQ432230	USA: NC: Guilford Co.	USA: MD: Montgomery Co.	Present	2
L. calcar	GQ870653, JQ432316, JQ432258, GQ872157, JQ432317, JQ432259, JQ432223, JQ432319, JQ432261, GQ870655, JQ432320, JQ432262, GQ872158, JQ432318, JQ432260	USA: MD: Frederick Co.	USA: TN: Carter Co.	Absent	9
L. euserratipalpe	JQ432321, JQ432263, GQ870656, JQ432322, JQ432264, GQ872160	USA: MD: Montgomery Co.	USA: MD: Frederick Co., USA: MD: Montgomery Co.	Absent	10
L. nigropalpi	JQ432323, JQ432265, JQ432224, JQ432324, JQ432266, JQ432225, JQ432325, JQ432267, JQ432226	USA: MD: Frederick Co.	USA: MD: Montgomery Co., USA: TN: Washington Co., USA: VA: Fairfax Co.	Absent	6
L. politum	JQ432326, JQ432268, JQ432227, JQ432327, JQ432269, JQ432228, JQ432328, JQ432270, JQ432229, JQ432329, JQ432271	USA: AR: Lawrence Co.	USA: MD: Montgomery Co.	Present	6
L. uxorium	JQ432339, JQ432281, JQ432235, JQ432338, JQ432280, JQ432236	USA: VA: Smythe Co.	USA: MD: Montgomery Co.	Absent	8
L. ventricosum	JQ432348, JQ432290, JQ432349, JQ432291, JQ432242, JQ432350, JQ432292, JQ432243	USA: TN: Blount Co.	USA: TN: Washington Co.	Present	5
L. verrucosum	JQ432351, JQ432293, JQ432244, JQ432347, JQ432289, JQ432241	USA: TN: Cumberland Co.	USA: MD: Montgomery Co., USA: TN: Washington Co.	Present	3
L. vittatum	JQ432333, JQ432275, JQ432232, GQ870651, JQ432334, JQ432276, GQ872155, JQ432335, JQ432277, JQ432233, JQ432336, JQ432278, JQ432234,GQ870652, JQ432337, JQ432279, GQ872156	USA: TN: Davidson Co.	USA: MD: Montgomery Co.	Absent	4

where F is the imposed bending force (in Newtons), D is vertical displacement of the beam at the point where F is applied (in meters), E is the elastic modulus of the material, I is the second moment of area of the beam, and L is the distance (in meters) between the base of the beam and the point where F is applied. E was assumed to be the same in all penes and was treated as a constant. I is a measure of architectural stiffness and reflects the amount and distribution of material around the flexural axis of a beam. It varies in proportion to d^4, where d is a characteristic length of an isometric system. We used the width of the propeltidium of the carapace between coxae I and II (d) as the characteristic length; the propeltidium is a single sclerite and is largely unaffected by nutritional or reproductive status of an adult specimen.

To determine the size correction for F, we solved Equation 2 for F by converting all other parameters to d^n by dimensional analysis:

$$[F_i] = DIL^{-3} = d^1 d^4 d^{-3} = d^2 \quad (3)$$

Thus, we size corrected F_{max} by dividing its measured value by the square of carapace width to obtain cF_{max}.

We obtained elastic efficiency R by dividing the area under the unloading portion of the hysteresis loop W_o (i.e., mechanical energy out) by the area under the corresponding loading portion of the loop W_i (i.e., mechanical energy in) (Fig. 3A, C, D). Given our assumptions of isometry and constant E (see above), no size correction for R was required.

T_{90} was the time (in seconds) required for the force of flexural resistance to undergo viscoelastic relaxation to 90% F_{max}. We did not attempt to correct T_{90} for size given the absence of a time dimension in Eq. 1. In cases where 90% F_{max} was not reached after 180 s, 180 s was used as the relaxation time. cF_{max} and T_{90} were log-transformed to minimize heteroscedasticity between dorsal, ventral and lateral bending and between sacculate and non-sacculate groups.

Data analysis.—We used phylogenetic comparative methods in statistical analysis to control for covariance due to shared evolutionary history. We established a phylogenetic framework by pruning a maximum clade credibility tree from a previous Bayesian-likelihood analysis of leiobunine phylogeny

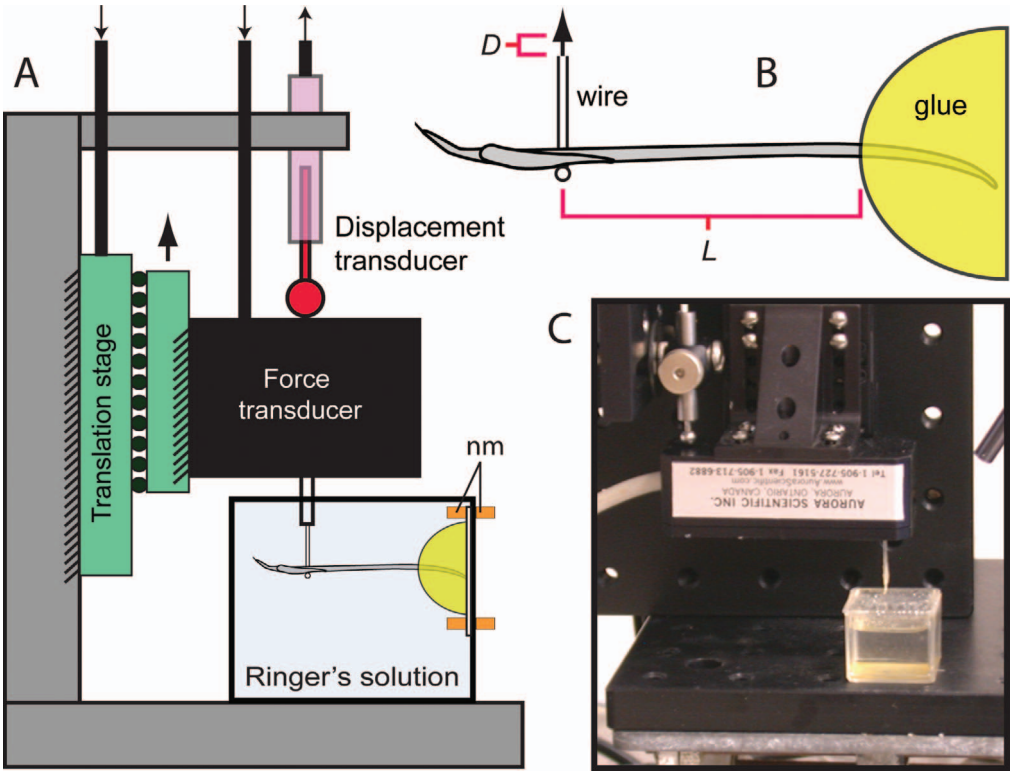

Figure 2.—Experimental apparatus. A. Forces associated with flexural displacement of harvestman penes were measured using a force transducer mounted vertically on a computer-driven translation stage, with vertical movement recorded by a displacement transducer. Penes were glued to a glass coverslip in cantilevered position. The mounted penis was placed in a bath of Ringer's solution and the coverslip was secured to the side of the bath with neodymium magnets (nm). A non-magnetic wire bent at 90° was attached to the input tube of the force transducer, brought into contact with the penis and used to bend the penis in three directions: dorsal, ventral and lateral. B. Lateral view of penis oriented for dorsal flexion. *L*, beam length, *D*, vertical displacement of beam (max. 0.05*L*). C. Photo of apparatus.

(Burns et al. 2013) to include only the 10 species examined here (Fig. 1A). The *geiger* package (Harmon et al. 2008), written in the statistical programming language R (R Development Core Team 2008), was used to evaluate evolutionary models for each variable. The models included Brownian motion, directional evolution (Brownian motion with a trend), Pagel's lambda (phylogenetic signal), kappa (punctuated equilibrium), and delta (time-dependent rates or comparable to early burst evolutionary model) (Pagel 1997, 1999). Evolutionary models were evaluated using the corrected Akaike information criterion (AICc), adjusted by the number of estimated parameters for each model. Model probability was determined by AICc weights (Burnham & Anderson 2004).

We performed phylogenetic principal components analyses using the R-based package *phytools* (Revell 2012) to explore covariation among mechanical variables. The predictions presented in the introduction anticipate positive covariation among variables that should be reflected in similarities in variable loadings and the placement of sacculate and non-sacculate species into separate clusters. Differences in mechanical variables between sacculate and non-sacculate groups were investigated further using phylogenetic multiple analysis of variance (pMANOVA) (Garland et al. 1993) as implemented in the *geiger* package. The Wilk's lambda test statistic and significance level were calculated for the data and for one million Brownian-motion simulations based on the evolutionary variance/covariance matrix estimated from the data across the phylogeny. Thus, model significance indicated by the standard MANOVA is supported by the commonality of the actual-data test statistic compared to a null distribution. We conducted Shapiro-Wilk's and Levene's tests (using the R package *asbio*; Aho 2014) on each variable to assess normality and homoscedasticity.

RESULTS

Models of evolution.—We used the fitContinuous function in the R package *geiger* to determine the best fit based on AICc for five potential models of evolution for each mechanical variable (Table 2). Most variables were best modeled by Brownian motion. This result was reinforced by maximum likelihood estimates of Pagel's lambda, which equaled or approached 1.0 for several traits across the three bending directions, including dorsal $\log T_{90}$, dorsal and lateral $\log cF_{max}$, and ventral and lateral R. A lambda value of 1.0 is considered equivalent to a Brownian motion evolutionary model (Boettiger et al. 2012) and indicates that covariance can be largely attributed to shared evolutionary history (i.e., length of shared branches.) Two mechanical variables had lower AICc scores for non-Brownian models; lateral $\log T_{90}$ was best modeled by the kappa branch transformation ($\kappa =$ 6.6E-214, AICc = 252.56) and lateral R was best modeled by the lambda branch transformation ($\lambda = 0.715$, AICc = 4.06). In both cases, the Brownian model had the next highest AIC

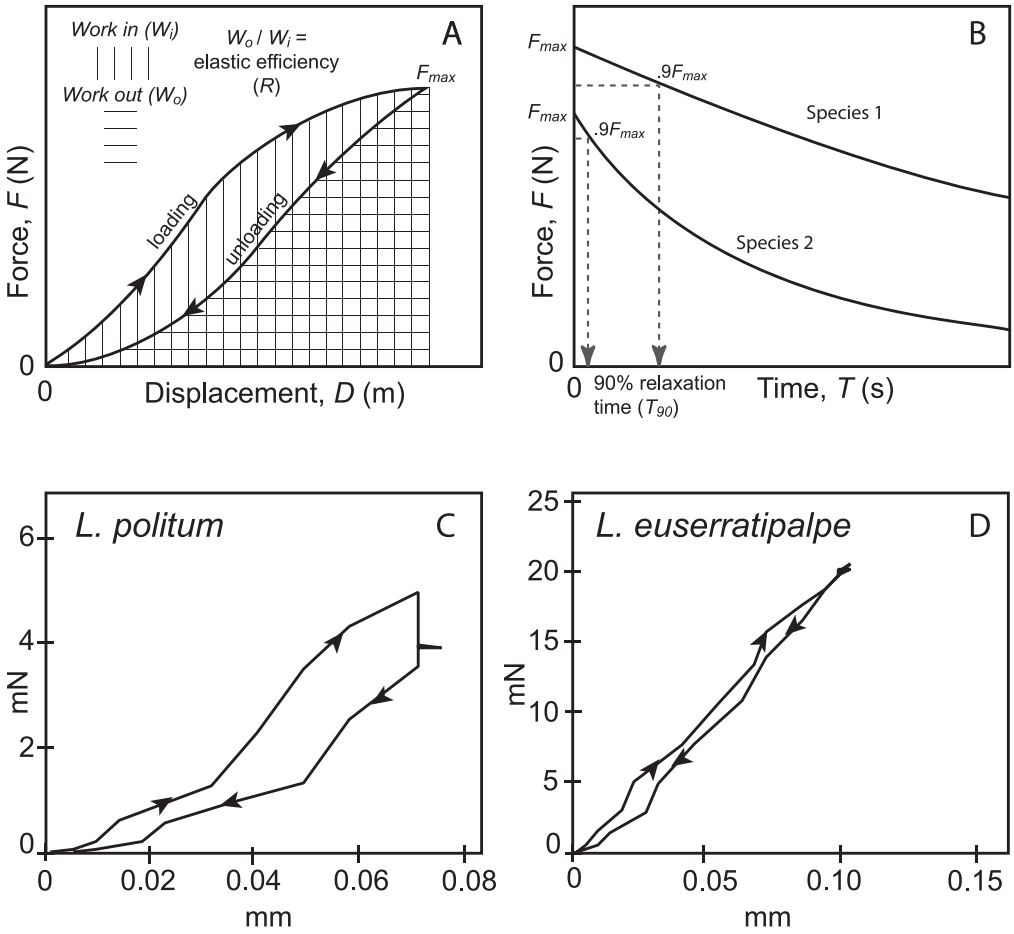

Figure 3.—Diagrammatic plots illustrating biomechanical variables and ventral sample data. A. Hysteresis loop showing parameters used to calculate elastic efficiency *R*. The work generated when a penis is loaded in flexion is proportional to the area under the loading curve (*Wi*). The work generated by the penis against the force transducer during re-extension (W_o) reflects the elastic energy stored in the penis. Thus, W_o/W_i equals *R*. B. Plot illustrating determination of T_{90}, the time required for the maximum force of flexural resistance F_{max} to relax to 90% F_{max}. We anticipated that a penis specialized for coercive interaction with females should have a higher F_{max}, T_{90} and *R* than penes adapted to accommodate female preferences. C. Hysteresis loop for ventral flexion in *Leiobunum politum* specimen (sacculate). D. Hysteresis loop for ventral flexion in a *L. euserratipalpe* specimen (non-sacculate, *calcar* species-group).

weight (lateral $T_{90} = 0.27$; lateral $R = 0.31$), indicating that the alternative model did not provide significant improvement over Brownian motion. However, it may be meaningful that the traits best modeled by the more-complex functions were both derived from lateral bending.

Exploring covariation in mechanical variables using principal components analysis.—We performed a phylogenetic principal components analysis using a multivariate lambda model of evolution to account for phylogenetic covariance due to species relatedness ($\lambda = 6.9E\text{-}5$, LogL $\lambda = 36.1$). Variable loadings are given in Table 3 and plotted alongside species scores in Fig. 4. Principal components 1 and 2 accounted for about 80% of total variance. Several mechanical variables for dorsal and ventral bending loaded highly on PC1, particularly dorsal and ventral logT_{90} and dorsal *R*. Variables associated with lateral bending tended to load more heavily on PC2.

Principal component 1 separated the *L. calcar* group from all other species, indicating that its members had comparatively high dorsal and ventral logT_{90}. Principal component 2 separated four sacculate species (*L. verrucosum, L. aldrichi, L. politum, L. bracchiolum*) into one cluster and the non-sacculate *vittatum* group (*L. vittatum*, *L. uxorium*) plus the sacculate *L. ventricosum* in another. The *ventricosum*/*vittatum* group was characterized by comparatively high lateral and ventral *R*, long lateral logT_{90}, and short dorsal and ventral logT_{90}.

Mechanical comparisons between sacculate and non-sacculate penes.—Results from group-mean comparisons using phylogenetic MANOVA are summarized in Fig. 5. No significant difference between sacculate and non-sacculate groups was found for *R* (Wilk's $\lambda = 0.33$, $F_{3,6} = 4.04$, model $P = 0.069$, phylogenetic $P = 0.68$) or logcF_{max} (Wilk's $\lambda = 0.7$, $F_{3,6} = 0.856$, model $P = 0.512$, phylogenetic $P = 0.19$) for any of the three flexural direction. High phylogenetic *P*-values for these models indicate that similar group means were achieved in most simulations, where phylogenetic branch lengths are randomly rescaled to allow greater potential change along longer segments.

There was a significant difference between sacculate and non-sacculate species in logT_{90} (Wilk's $\lambda = 0.26$, $F_{3,6} = 5.77$, model $P < 0.05$) (Fig. 5D), with non-sacculate penes taking

Table 2.—Evolutionary model selection for body size and mechanical force traits. Akaike information criterion corrected for small sample size ($AICc_{wt}$) standardized weights mechanical reproductive traits. Models included Brownian motion (random walk), Directional (Brownian motion with a trend), kappa (punctuated equilibrium), lambda (phylogenetic signal), and delta (time-dependence) (Pagel 1999, 1997). Unstandardized weights were calculated with the equation $AICc_{wt} = e^{((AIC_{minimum} - AIC_i)/2)}$ (Burnham & Anderson 2004). Preferred model (greatest $AICc_{wt}$) is indicated with asterisk (*).

	Model				
Mechanical variable	Brownian ($AICc_{wt}$)	Directional ($AICc_{wt}$)	kappa ($AICc_{wt}$)	lambda ($AICc_{wt}$)	delta ($AICc_{wt}$)
Elastic efficiency (R)					
Dorsal	*0.4098	0.0719	0.1628	0.1553	0.2002
Ventral	*0.5729	0.0768	0.1173	0.1141	0.1189
Lateral	0.3069	0.0528	0.1432	*0.3596	0.1373
90%-relaxation time (T_{90})					
Dorsal	0.6216	0.1962	0.0564	0.0564	0.0694
Ventral	0.5843	0.0851	0.0536	0.1017	0.1752
Lateral	0.2695	0.0453	*0.4407	0.1377	0.1067
Maximum experimental displacement force (F_{max})					
Dorsal	*0.6211	0.0866	0.0882	0.0563	0.1476
Ventral	*0.4059	0.0720	0.1293	0.1742	0.2185
Lateral	0.6525	0.0823	0.0839	0.0592	0.1221

significantly more time to reach 90% of F_{max}. However, this result was not robust to evolutionary data replication (phylogenetic $P = 0.7815$), indicating that a significant group difference based on sac presence would not be found under the majority of $\log T_{90}$ simulations with identical evolutionary conditions. Tests of data normality and heteroscedasticity indicated that all variables were normally distributed, but there were unequal variances between sacculate and non-sacculate species for many variables, primarily those measured during dorsal flexion (dorsal $\log cF_{max}$: $F_{1,8} = 16.7$, $P < 0.01$; $\log T_{90}$: $F_{1,8} = 8.61$, $P < 0.05$). Heteroscedasticity within the non-sacculate category is consistent with results from the principal components analysis (Fig. 4), where the *vittatum* group tended to cluster with the sacculate species, and not with the non-sacculate *calcar* group.

Although phylogenetic simulation did not identify a significant difference in $\log T_{90}$ between sacculate and non-sacculate species, we performed three follow-up phylogenetic univariate tests comparing means of dorsal, ventral, and lateral $\log T_{90}$. We found significantly longer relaxation times for dorsal ($F_{1,8} = 5.16$, $P < 0.05$) and lateral ($F_{1,8} = 19.21$, $P < 0.001$) bending in non-sacculate species, and a similar, though non-significant, trend for higher ventral $\log T_{90}$ ($F_{1,8} = 0.639$, $P = 0.78$). These results demonstrate significant differentiation of elastic responses in penile cuticle between sacculate and non-sacculate species.

Table 3.—Trait loadings of phylogenetic principal component analyses, eigenvalues, and percent variance explained by first two principal components (PC).

Mechanical variable	PC 1	PC 2
Elastic efficiency (R)		
Dorsal	−0.783	0.254
Ventral	−0.661	−0.655
Lateral	−0.476	−0.811
90% relaxation time (T_{90})		
Dorsal	−0.977	−0.018
Ventral	−0.741	−0.008
Lateral	−0.566	−0.775
Max. resistance force(F_{max})		
Dorsal	−0.726	0.579
Ventral	−0.829	0.452
Lateral	−0.596	0.481
Eigenvalues	4.67	2.52
% Variance	51.89	28.05

Following the result from the phylogenetic principal components analysis, which separated non-sacculate species into *vittatum*/*ventricosum* and *calcar* groups, we repeated the phylogenetic MANOVA with three group-mean comparisons, separating trait values by sacculate, *vittatum*/*ventricosum*, and *calcar* group membership. This model yielded significant differences in all three variables (R: Wilk's $\lambda = 0.05$, $F_{6,10} = 5.76$, model $P < 0.01$; $\log cF_{max}$: Wilk's $\lambda = 0.116$, $F_{6,10} = 3.23$, model $P < 0.05$), although in phylogenetic simulation only $\log T_{90}$ was found to be significantly different between groups (Wilk's $\lambda = 0.0079$, $F_{6,10} = 17.107$, model $P < 0.0001$, phylogenetic $P < 0.01$). A phylogenetic ANOVA with Holm-Bonferroni *posthoc* test to compare bending directions for each of the three variables identified significantly higher dorsal $\log T_{90}$ ($F_{1,7} = 20.83$, $P < 0.05$) in the *calcar* group as compared to the two other groups, as well as a hierarchy of significant differences in lateral $\log T_{90}$ ($F_{1,7} = 43.52$, $P < 0.01$) between the sacculate, *vittatum*/*ventricosum,* and *calcar* groups (Fig. 5). Using this method, we additionally found significant differences between the sacculate and *calcar* groups in ventral R ($F_{1,7} = 14.06$, $P < 0.05$) and between the *calcar* and *vittatum* groups in dorsal $\log cF_{max}$ ($F_{1,7} = 18.05$, $P < 0.05$) and ventral $\log cF_{max}$ ($F_{1,7} = 15.18$, $P < 0.05$). Values of R and $\log cF_{max}$ for the *vittatum* + *L. ventricosum* and sacculate groups were statistically indistinguishable.

DISCUSSION

Previous work on the evolution of reproductive structures and mating systems in *Leiobunum* and related taxa (Burns & Shultz 2015) identified the coevolution of relative maximum

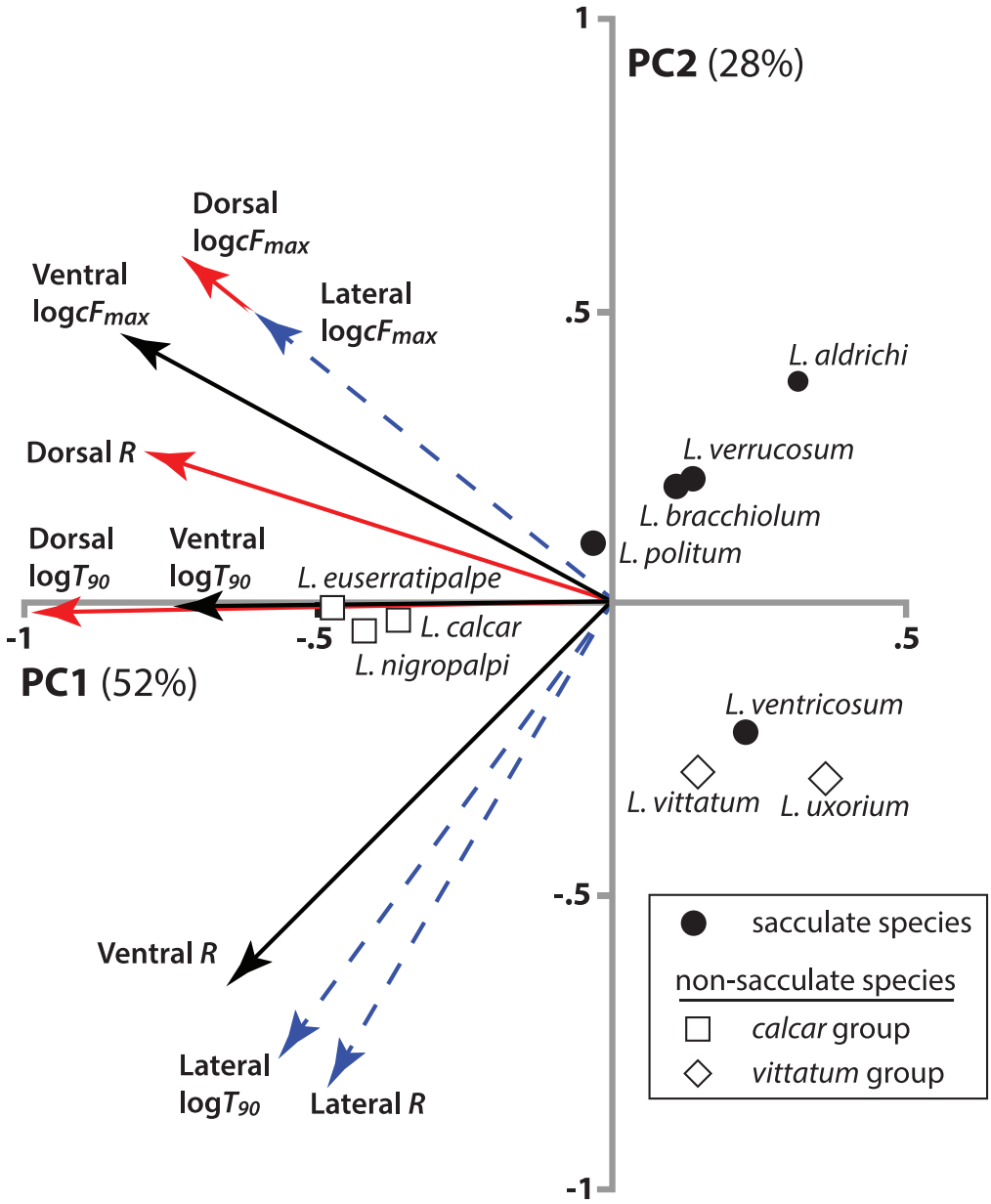

Figure 4.—Phylogenetic principal components analysis of mechanical force data. The pPCA, applied to dorsal, ventral, and lateral measures of maximum flexural resistance (log cF_{max}), elastic efficiency (R) and time to 90% relaxation of F_{max} (logT_{90}). Principal components 1 and 2 together account for 80% of total data variance. Trait loadings are indicated by arrows, color coded by flexural orientation. Non-sacculate species indicated by white shapes—squares for the *calcar* group, diamonds for the *vittatum* group—and sacculate species indicated by black circles.

force produced by the penis protractor muscle and by the closure of the female genital operculum. These relative forces are higher in non-sacculate species, which suggests that greater mechanical forces are produced and resisted in non-sacculate forms. Following this line of evidence, we tested our expectation that presence and absence of penile nuptial gift sacs in *Leiobunum* correspond to differences in the flexural biomechanics of the penis shaft. We predicted that penes in sacculate and non-sacculate species differ in the magnitudes of three biomechanical variables—maximum resistance to experimental penile flexure (F_{max}), efficient storage of elastic energy (R) for use in restoring the flexed penis to the resting state, and persistence of the restoring force during static flexion (T_{90})—with the non-sacculate species having higher values. We obtained these values for each of three biologically relevant bending directions, and used modern phylogenetic comparative methods to find covariation between nuptial gift sac presence and biomechanical specialization. Our success in doing so demonstrates that biomechanical data can be obtained from arthropod genitalia and may be useful in resolving functionally distinct groups.

Results from phylogenetic MANOVA showed no significant differences between sacculate and non-sacculate species groups, except perhaps in T_{90}. These findings are consistent with those obtained from multivariate analysis based on measurements and functional inferences from static reproduc-

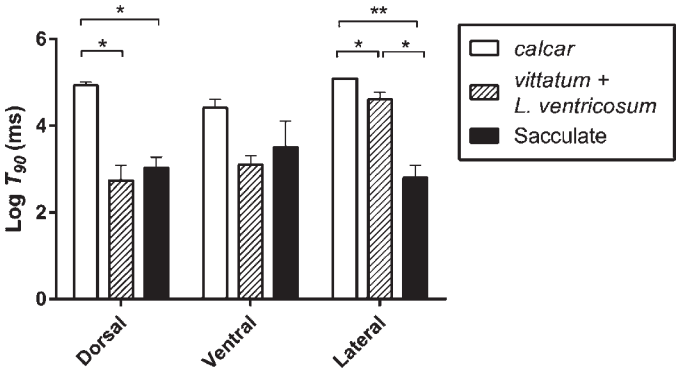

Figure 5.—Phylogenetic ANOVA results for logT_{90}. Bar graph results summarize phylogenetic ANOVA tests comparing the $\log_{10}$-transformed viscoelastic relaxation times of penes displaced dorsally, ventrally, and laterally for sacculate, *vittatum*/*ventricosum* and *calcar* clusters. Bars are group means plus standard error for sacculate (black), *vittatum*/*ventricosum* (hatched lines) and *calcar*-group (white) species for each of three bending aspects. Asterisks indicate significance level of between-group comparisons ('*' $P_t < 0.05$; '**' $P_t < 0.01$).

tive morphology (Burns & Shultz 2015). Specifically, canonical correlation, bivariate correlation and principal components analyses placed leiobunine species along a continuum of "antagonistic specialization" in which sacculate species dominated one end and non-sacculate species dominated the other, with a broad region of overlap that precluded classification into distinct sacculate/enticement and non-sacculate/coercion groups. In contrast, results from the current study differ in that pPCA (Fig. 4) appeared to recover three species clusters rather than a single cluster or continuum. PC1 may represent the antagonistic potential associated with dorsal and ventral penile flexure, with higher values toward the left side of the plot. This axis separates the non-sacculate *calcar* group, with high antagonistic potential, from all other species, including the non-sacculate *vittatum* species-group. Furthermore, PC2 appears to correspond to the antagonistic potential associated with lateral flexure and separates the *vittatum* species-group plus the sacculate *L. ventricosum* from the remaining sacculate taxa.

More specifically, PCA results from our current study indicate that penes in the *calcar* group offer greater resistance to dorsal and ventral flexure relative to body size (cF_{max}) than those of the other species examined. Further, relatively more elastic energy is stored in the flexed penis for use in flexural resistance during re-extension (R), and the restoring force persists for a longer time (T_{90}). This result is consistent with initial predictions, but was not found in the *vittatum* group, and the results were thus inconsistent with predictions about non-sacculate penes generally. The species outside the *calcar* group were separated primarily by factors associated with lateral flexure, with sacculate species (except *L. ventricosum*) having greater resistance to lateral flexion relative to body size than the *vittatum*/*ventricosum* cluster. The relatively greater flexural compliance of the *vittatum*/*ventricosum* cluster may be attributed to the greater relative length (L) of penes and the low second moment of area (I) of the penis shaft in the *vittatum* group, which is narrow and circular in cross section rather than wide and dorsoventrally compressed as in sacculate species (see Eq. 1; Fig. 1). In contrast, lateral bending in the penes of the *vittatum*/*ventricosum* cluster showed viscoelastic properties higher than those of most sacculate species (i.e., with higher energy storage and longer relaxation times).

Given the rather low sample size and high experimental variance in some of our data, it is premature to conclude that the three clusters recovered by PCA correspond to functional groups or mating strategies. Furthermore, we modeled displacement assuming penes were the equivalent of a beam, although unlike standard beams, penes of these species are not consistent in width across length. While we did not vary the application site of forces, we could expect incremental changes in second moment of area (I) as the site of displacement (L) is repositioned. However, the combination of mechanical properties within each cluster, together with other morphological and behavioral observations, may offer new insights and testable hypotheses. Specifically, we propose that the *calcar* group still exemplifies an antagonistic mating system in which male coercion and forced penetration have played an important role in shaping genitalic morphology and biomechanics. This conclusion is consistent with the robust pedipalps in males that are used to clasp the female during mating and a sclerotized latch mechanism at the pregenital opening of females (Ingianni et al. 2011). The cluster of four sacculate species may represent a mating system dominated by male enticement of females. Members of this group have short but dorsoventrally flexible penes with gift-bearing sacs. The penes are poorly designed for imposing significant mechanical forces and, in fact, are mounted on a fluid-filled turret (haematodocha) during mating (Fig. 1) that would tend to accommodate rather than resist female movements. In addition, females of the species group have no special elaboration of the pregenital opening that might resist forceful penetration, although larger body size alone may be a sufficient defense. Finally, we speculate that the genitalic features of the mixed *vittatum*/*ventricosum* cluster could reflect specializations that allow females to coerce prolonged delivery of nuptial gifts from males by entrapping or imposing possible damage to the penis (as in Kuriwada & Kasuya 2011). Such a system would combine elements of enticement by the male and antagonism by the female and might thus account for the intermediacy between enticement and antagonism revealed in our previous study (Burns & Shultz 2015).

A few other lines of evidence are consistent with female coercion of males via penis entrapment. Specifically, recent behavioral analyses of mating in *L. vittatum* from Wisconsin indicate that females may regulate the duration of mating contact, in part, by resisting male attempts at separation (Fowler-Finn et al. 2014) and that males sometimes show signs of physiological exhaustion after mating (K. Fowler-Finn, pers. comm.). Interestingly, male *L. vittatum* from Massachusetts have been found with no other damage than a broken penis (Fig. 6A-C), which is consistent with persistent penile entrapment by the female. Although we previously characterized the sclerotized sterno-opercular mechanism in female *L. vittatum* as a pregenital barrier (Burns et al. 2013; Burns & Shultz 2015), the pregenital mechanism could also be used for entrapping the penis. In contrast, our own video-based observations of mating in *L. ventricosum* show no obvious signs of female coercion during mating. However, *Leiobunum*

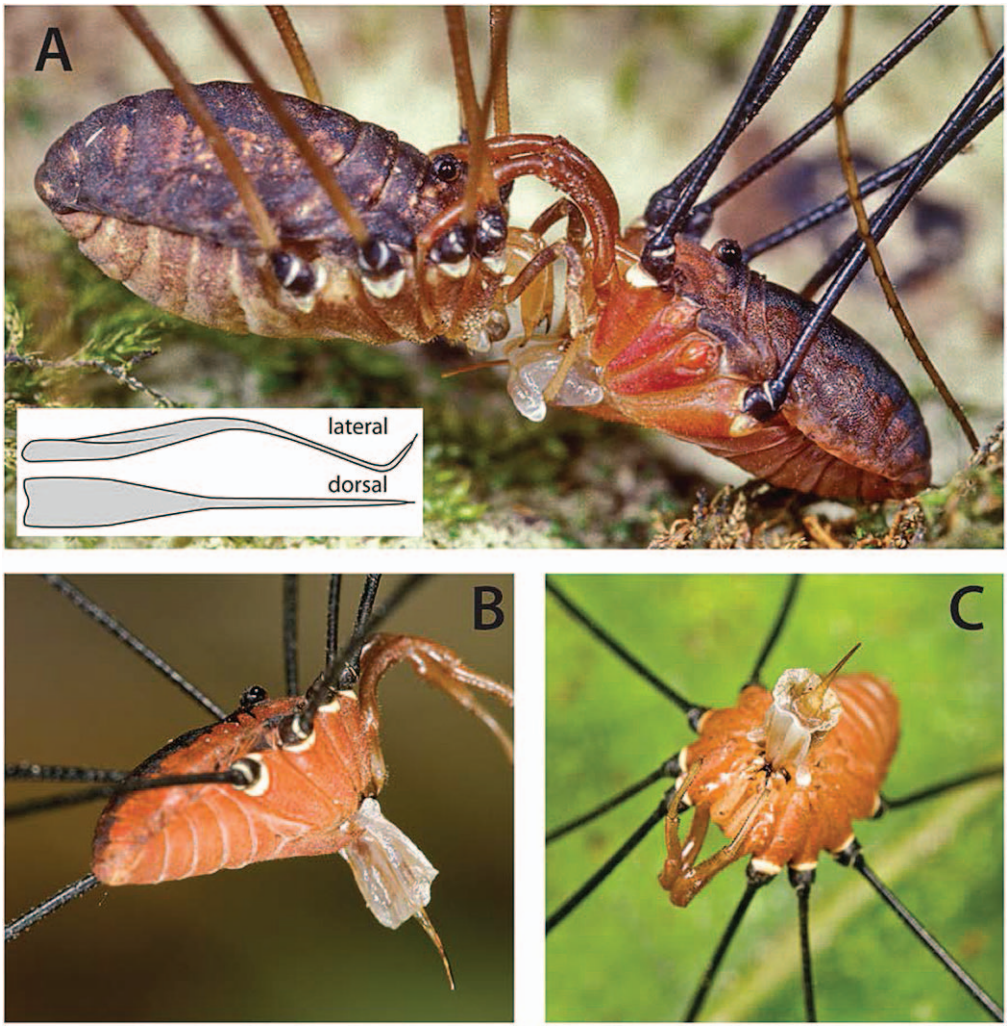

Figure 6.—Male *Leiobunum vittatum* found with broken penes, suggesting mechanical damage incurred during mating. A. Mating *L. vittatum* (female left, male right). Male clasps female coxa II (as in Fig. 1C) with damaged penis extended. Female palpates male haematodocha. Lateral and dorsal drawings of *L. vittatum* penis are inset. B. Ventrolateral view of male *L. vittatum* with broken penis. C. Ventral view of same male. In both examples, male penis is broken at the upturned glans portion. All pictures courtesy of Joe Warfel/Eighth Eye Photography, Massachusetts, USA.

holtae McGhee, 1977 (not included in the present study), a derived species that appears to have evolved from *L. ventricosum*-like ancestors (Burns et al. 2012), is morphologically similar to *L. vittatum* in having a long, thin non-sacculate penis. In addition, the female pregenital opening has a large, horizontally-arranged opercular plate that can be pressed against a large sternite dorsally. Again, this mechanism could be interpreted as either a barrier (which seems substantially overdesigned given the apparent compliance of the penis) or a penis trap. It is therefore possible that the condition in *L. holtae* evolved from a less extreme form of female coercion that may be practiced by *L. ventricosum*. Testing this speculative hypothesis will require new, intensive studies of mating behavior and functional morphology.

ACKNOWLEDGMENTS

We are grateful to Mary E.L. Burns and the attendees of the 2013 American Arachnological Society held at East Tennessee State University in Johnson City, TN, for their assistance in specimen collection and to Joe Warfel for photographs of *L. vittatum*. We additionally thank Dan Gruner, David Hawthorne, Sara Bergbreiter, Priscila Chaverri, and four anonymous reviewers for discussion of the manuscript. MB was supported by the University of Maryland and GRF, DDIG, and PRFB grants from the National Science Foundation. JWS was supported by the Maryland Agricultural Experiment Station. The funders had no role in study design, data collection and analysis, decision to publish, or preparation of the manuscript.

LITERATURE CITED

Ah-King, M., A.B. Barron & M.E. Herberstein. 2014. Genital evolution: Why are females still understudied? PLoS Biol 12(5): e1001851. doi: 10.1371/journal.pbio.1001851.

Aho, K. 2014. Foundational and applied statistics for biologists using R. CRC/Taylor and Francis, Boca Raton.

Albo, M.J., T. Bilde & G. Uhl. 2013. Sperm storage mediated by

cryptic female choice for nuptial gifts. Proceedings of the Royal Society B 280:e20131735. doi:10.1098/rspb.2013.1735.
Boettiger, C., G. Coop & P.L. Ralph. 2012. Is your phylogeny informative? Measuring the power of comparative methods. Evolution 66:2240–2251.
Bonduriansky, R. & T. Day. 2003. The evolution of static allometry in sexually selected traits. Evolution 57:2450–2458.
Brennan, P.L.R., C.J. Clark & R.O. Prum. 2010. Explosive eversion and functional morphology of the duck penis supports sexual conflict in waterfowl genitalia. Proceedings of the Royal Society B 277(1686): doi: 10.1098/rspb.2009.2139.
Brennan, P.L., R.O. Prum, K.G. McCracken, M.D. Sorenson, R.E. Wilson & T.R. Birkhead. 2007. Coevolution of male and female genital morphology in waterfowl. PLoS ONE 2(5):e418. doi: 10.1371/journal.pone.0000418.
Burnham, K.P. & D.R. Anderson. 2004. Multimodal inference: understanding AIC and BIC in model selection. Sociological Methods and Research 33:261–304.
Burns, M.M. & J.W. Shultz. 2015. Biomechanical diversity of mating structures among harvestmen species is consistent with a spectrum of precopulatory strategies. PLoS ONE 10(9):e0137181. doi: 10.1371/journal.pone.0137181.
Burns, M., M. Hedin & J.W. Shultz. 2012. Molecular phylogeny of the leiobunine harvestmen of eastern North America (Opiliones: Sclerosomatidae: Leiobuninae). Molecular Phylogenetics & Evolution 63:291–298.
Burns, M.M., M. Hedin & J.W. Shultz. 2013. Comparative analyses of reproductive structures in harvestmen (Opiliones) reveal multiple transitions from courtship to precopulatory antagonism. PLoS ONE 8(6):e66767. doi:10.1371/journal.pone.0066767.
Cassidy, E.J., E. Bath, S.F. Chenoweth & R. Bonduriansky. 2014. Sex-specific patterns of morphological diversification: Evolution of reaction norms and static allometries in Neriid flies. Evolution 68:368–383.
Cayetano, L., A.A. Maklakov, R.C. Brooks & R. Bonduriansky. 2011. Evolution of male and female genitalia following release from sexual selection. Evolution 65:2171–2183.
Crosby, C.R. & S.C. Bishop. 1924. Notes on the Opiliones of the southeastern United States with descriptions of new species. Journal of the Elisha Mitchell Scientific Society 40:8–26.
Day, T. & K.A. Young. 2004. Competitive and facilitative evolutionary diversification. BioScience 54:101–109.
Eberhard, W.G. 1996. Female Control: Sexual Selection by Cryptic Female Choice. Princeton Univ. Press, Princeton.
Edwards, D.L. & L.L. Knowles. 2014. Species detection and individual assignment in species delimitation: can integrative data increase efficacy? Proceedings of the Royal Society B 281 (1777): doi: 10.1098/rspb.2013.2765.
Fowler-Finn, K.D., E. Triana & O.G. Miller. 2014. Mating in the harvestman *Leiobunum vittatum* (Arachnida: Opiliones): from premating struggles to solicitous tactile engagement. Behaviour 151:1663–1686.
Garland, T., A.W. Dickerman, C.M. Janis & J.A. Jones. 1993. Phylogenetic analysis of covariance by computer simulation. Systematic Biology 42:265–292.
Harmon, L.J., J.T. Weir, C.D. Brock, R.E. Glor & W. Challenger. 2008. GEIGER: investigating evolutionary radiations. Bioinformatics 24:129–131.
Hosken, D.J. & P. Stockley. 2004. Sexual selection and genital evolution. Trends in Ecology and Evolution 19:87–93.
Ingianni, E., C.R. McGhee & J.W. Shultz. 2011. Taxonomy of the *Leiobunum calcar* species-group (Opiliones, Sclerosomatidae, Leiobuninae). Journal of Arachnology 39:454–481.
Koch, C.L. 1839. Übersicht des Arachnidensystems. Zweites Heft, Nürnberg.
Kokko, H., R. Brooks, M.D. Jennions & J. Morley. 2003. The evolution of mate choice and mating biases. Proceedings of the Royal Society of London B 270:653–664.
Kuriwada, T. & E. Kasuya. 2011. Nuptial gifts protect male bell crickets from female aggressive behavior. Behavioral Ecology 23:302–306. doi: 10.1093/beheco/arr186.
Leonard J.L. & A. Córdoba-Aguilar, eds. 2010. The Evolution of Primary Sexual Characters in Animals. Oxford University Press, Oxford.
Machado, G., G.S. Requena, C. Toscano-Gadea, E. Stanley & R. Macías-Ordóñez. 2015. Male and female mate choice in harvestmen: General patterns and inferences on the underlying processes. Pp. 169–201. *In* Cryptic Female Choice in Arthropods: Patterns, Mechanisms, and Prospects. (A.V. Peretti, A. Aisenberg, eds.). Springer International Publishing, Cham, Switzerland.
McGhee, C.R. 1977. The *politum* group (bulbate species) of *Leiobunum* (Arachnida: Phalangida: Phalangiidae) of North America. Journal of Arachnology 3:151–163.
Márquez, E.J. & L.L. Knowles. 2007. Correlated evolution of multivariate traits: detecting co-divergence across multiple dimensions. Journal of Evolutionary Biology 20:2334–2348.
Masly, J.P. & Y. Kamimura. 2014. Asymmetric mismatch in strain-specific genital morphology causes increased harm to *Drosophila* females. Evolution 68:2401–2411.
Pagel, M. 1997. Inferring evolutionary processes from phylogenies. Zoologica Scripta 26:331–348.
Pagel, M. 1999. Inferring the historical pattern of biological evolution. Nature 401:877–884.
Parker, G.A., C.M. Lessells & L.W. Simmons. 2013. Sperm competition games: a general model for precopulatory male-male competition. Evolution 67:95–109.
R Development Core Team. 2008. R: A language and environment for statistical computing. R Foundation for Statistical Computing, Vienna, Austria. Accessed 16 March 2014. Online at http://www.R-project.org
Revell, L.J. 2012. Phytools: An R package for phylogenetic comparative biology (and other things). Methods in Ecology and Evolution 3:217–223.
Sánchez, V., B.E. Hernández-Baños & C. Cordero. 2011. The evolution of a female genital trait widely distributed in the Lepidoptera: comparative evidence for an effect of sexual coevolution. PLoS ONE 6(8):e22642. doi: 10.1371/journal.pone.0022642.
Say, T. 1821. An account of the Arachnides of the United States. Journal of the Academy of Natural Sciences of Philadelphia 2:59–82.
Tanabe, T. & T. Sota. 2013. Both male and female novel traits promote the correlated evolution of genitalia between the sexes in an arthropod. Evolution 68:441–452.
Vincent, J., 2012. Structural Biomaterials. 3rd edition. Princeton University Press, Princeton.
Vogel, S. 2003. Comparative Biomechanics. Princeton University Press, Princeton.
Weed, C.M. 1889. A descriptive catalogue of the Phalangiinae of Illinois. Bulletin of the Illinois State Laboratory of Natural History 3:79–97.
Weed, C.M. 1893. A synopsis of the harvest-spiders (Phalangiidae) of South Dakota. Transactions of the American Entomological Society 20:285–292.
Wood, H.C. 1868. On the Phalangeae of the United States of America. Proceedings of the Essex Institute 6:10–40.

Manuscript received 15 December 2015, revised 22 February 2016.